Exon, N.F., Kennett, J.P., and Malone, M.J. (Eds.)
Proceedings of the Ocean Drilling Program, Scientific Results Volume 189

9. Integrated Age Models for the Early Oligocene–Early Miocene, Sites 1168 and 1170–1172[1]

Helen A. Pfuhl[2] and I. Nicholas McCave[3]

ABSTRACT

The aim of this study is to assess the viability of age models based on shipboard and postcruise bio- and magnetostratigraphic datums, as of August 2002, using independently derived control points. The control points are based on matching between-site trends in stable isotope records, carbonate content, and weight percent sand. Site 1170 on the western South Tasman Rise has a good record of magnetic reversals, which suggests a hiatus prior to ~30 Ma (early Oligocene) relating to the Marshall Paraconformity, followed by strongly reduced sedimentation in the late Oligocene. Preservation of the Mi-1 event at this site is evidence for continued sedimentation across the Oligocene/Miocene boundary. Correlation of the Mi-1a event to the record at Site 1090 on the Agulhas Ridge confirms the usefulness of the magnetostratigraphic record at this site. However, the timing of the Mi-1 event at Site 1170 appears different from that at Site 1090, but is constrained by four magnetic reversals. At Site 1171 additional control points are consistent with biostratigraphic datums. Site 1172 is marked by the lowest sedimentation rates of all sites. Additional control points before 22 Ma are more consistent with the biostratigraphy than with the magnetostratigraphy. At Site 1168 we suggest that the magnetic reversal record MR1 provides the best match with the biostratigraphy and additional control points, as well as changes in the biogenic and lithogenic composition of the sedimentary record.

[1]Pfuhl, H.A., and McCave, I.N., 2003. Integrated age models for the early Oligocene–early Miocene, Sites 1168 and 1170–1172. *In* Exon, N.F., Kennett, J.P., and Malone, M.J. (Eds.), *Proc. ODP, Sci. Results,* 189, 1–21 [Online]. Available from World Wide Web: <http://www-odp.tamu.edu/publications/189_SR/VOLUME/CHAPTERS/108.PDF>. [Cited YYYY-MM-DD]
[2]Max Planck Institute for Biogeochemistry, Hans Knöll Strasse 10, 07745 Jena, Germany.
hapfuhl@yahoo.com
[3]University of Cambridge, Department of Earth Sciences, Downing Street, Cambridge CB2 3EQ, United Kingdom.

Initial receipt: 2 December 2002
Acceptance: 9 July 2003
Web publication: 12 November 2003
Ms 189SR-108

The late Eocene/early Oligocene Marshall Paraconformity (base = ~33 Ma at the type location) is evident at Sites 1170–1172, and low sedimentation rates occur at the two eastern sites (1171 and 1172) in the early Oligocene. A change in sedimentation just after the early–late Oligocene transition appears to reduce rates at Site 1170 and strongly affect the biogenic composition of sediments at Site 1168, which is less exposed to the flow of the Antarctic Circumpolar Current. The Oligocene–Miocene transition finally is marked by reduced sedimentation at Sites 1170–1172, but a relatively stronger decrease is noticeable at Site 1168. Above this boundary sedimentation rates are identical at Sites 1168 and 1170 above 21.5 Ma and at Sites 1171 and 1172 above 17 Ma.

APPROACH

A robust age model is essential to evaluate the changes in the hydrographic and sedimentary regime across the Oligocene/Miocene boundary (OMB) (Pfuhl et al., in press). Combined biostratigraphic and magnetostratigraphic age models for Ocean Drilling Program (ODP) Sites 1168 and 1170–1172, as of August 2002, were used in an initial comparison between sites. However, close study of records of percent $CaCO_3$, weight percent sand (>63 µm), and stable oxygen and carbon isotopes (bulk sediment and benthic foraminifers) provides additional information that is crucial in recognizing hiatuses, especially the Marshall Paraconformity in the early Oligocene (~32–29 Ma) (Fulthorpe et al., 1996) and sedimentary sequences. A detailed lithologic description of Sites 1168 and 1170–1172 (Fig. F1) is given in the Leg 189 *Initial Reports* volume (Exon, Kennett, Malone, et al., 2001).

F1. Map of drill sites (Site 1169 was abandoned), p. 10.

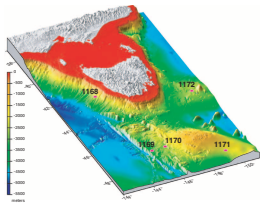

As a first step we attempt to correlate the benthic stable isotope records from Site 1170, with special focus on the Mi-1 and Mi-1a events (Miller et al., 1985) with those at Site 1090 (Billups et al., 2002) on the Agulhas Ridge south of Africa. A second step is to compare the results with the bio- and magnetostratigraphic data as of August 2002, but also see the study of **Stickley et al.** (this volume) and additional information on hiatuses/condensed sections or changes in sedimentation rate that are indicated by the measurements obtained during postcruise work (this study and Pfuhl et al., in press). The revised age model for Site 1170 incorporates the best fit between additional control points (this study) and the biomagnetostratigraphy (as of August 2002). This age model forms the basis for paleoceanographic correlation of Sites 1170–1172 and development of individual age models using the same overall approach as at Site 1170. In a final step we identify additional control points for Site 1168, which differs in its location on the continental margin from the open-ocean situation of Sites 1170–1172. A more recent version of the age models is presented by Pfuhl et al. (in press); however, the principles outlined here remain unchanged.

METHODS

Sites 1170–1172

Carbonate Content and Stable Isotope Composition

Bulk sediments from Sites 1170–1172 were analyzed for their carbonate content and stable isotope composition in an Analytical Precision

AP2003 mass spectrometer. Benthic isotope measurements were performed on ~10 specimens of *Cibicidoides mundulus* (in very rare cases on a mix of *Cibicidoides bradyi* and *Cibicidoides kullenbergi*) from the >212-µm size range. This genus is generally accepted as living within the sediment surface (0–1 cm), although *C. bradyi* might prefer a slightly more infaunal habitat. Analyses were performed using standard procedures for Prism mass spectrometers. Precision is better than ±0.06‰ for $\delta^{13}C$, ±0.10‰ for $\delta^{18}O$, and ±2% for carbonate. All stable isotope results were calibrated to the international standard Vienna Pedee belemnite through standard laboratory carbonates including correction for vital effects (Shackleton and Hall, 1997). A number of outlying measurements were subjected to repeat analysis. All measurements were performed at the Godwin Laboratory, Cambridge University.

Site 1168

Carbon Content

Fine-fraction carbon content (C_{total}) was measured by CHN analysis in a Carlo Erba EA1106 at the Godwin Laboratory, Cambridge University, UK. Additional measurements of total carbon and inorganic carbon content (TIC) were performed in an Elementar VarioMAX at the Max Planck Institute for Biogeochemistry, Jena, Germany. Samples for inorganic carbon content were combusted at ~400°C for 16 hr, as combustion of only 4 hr did not remove all nitrogen. In order to use both measurements of C_{total} we calculated a linear regression based on 32 parallel measurements from various intervals at Site 1168, arriving at a regression coefficient of $R^2 = 0.925$. All CHN measurements were subsequently converted to VarioMAX-equivalent values of C_{total} ($y = 0.9229x + 0.2674$), where y = VarioMAX-equivalent C_{total} and x = CHN value of total C. Total organic carbon (TOC) was approximated by

$$TOC = C_{total} - TIC.$$

Benthic Stable Isotope Composition

Four to eight *C. mundulus* specimens from the >150-µm size fraction were analyzed in VG Optima or Prism gas-source mass spectrometers at the University of California, Santa Cruz. All values are reported in permil notation relative to Vienna Peedee belemnite standard, with $\delta^{18}O$ measurements including a correction for vital effects (+0.5‰) (Shackleton and Hall, 1997). Analytical precision for both $\delta^{13}C$ and $\delta^{18}O$ averaged better than 0.1‰. No interlaboratory corrections were applied, as these are usually constant and should not affect our interpretations; however, we do concede that these offsets exist.

Faunal and Lithogenic Reconnaissance

Faunal and lithogenic reconnaissance is based on random order inspection of the >63-µm fraction at 75- to 300-cm resolution. We distinguished between

4 = common/dominant,
3 = frequent,
2 = present,

1 = rare, and
0 = absent (0),

the same scheme as applied in shipboard benthic foraminiferal studies at 9-m resolution (Exon, Kennett, Malone, et al., 2001).

RESULTS

All ages given in this study are based on Cande and Kent (1992; 1995) (CK95) unless stated otherwise (i.e., the OMB is placed at 23.8 Ma). Although the astronomically tuned age of the OMB is 22.9 Ma (Shackleton et al., 2000), the older Oligocene part of the section does not have a revised age scale; thus, we prefer to stick with CK95 for the time being. Data in the older parts are available only at low resolution (identified by gray backgrounds in figures), whereas resolution in the younger parts is 75 cm for Site 1168, 20 cm for Sites 1170 and 1171, and 10 cm for Site 1172. All biomagnetostratigraphic datums (as of August 2002) and additional control points used for our age models are listed in Table T1 (see also **Stickley et al.,** this volume).

T1. Fossil, magnetic reversal, and additional datums, p. 21.

Site 1170

The benthic stable isotope records of Site 1170 on the South Tasman Rise and Site 1090 on the Agulhas Ridge, both located in the Southern Ocean, suggest some similarities despite different paleolatitudes. The benthic isotope record for Site 1090 was established by Billups et al. (2002), who developed their age model by matching the excellent magnetic polarity stratigraphy to the geomagnetic polarity timescale of CK95. A comparison of their results with the astronomically tuned record of Shackleton et al. (2000) yielded a constant offset of ~900 k.y. between the two approaches. We focus on the timing of the Mi-1 and Mi-1a event in the benthic $\delta^{18}O$ records, which are identifiable at both sites despite relatively low sedimentation rates (Fig. F2A).

F2. Comparison of Mi-1a and Mi-1 events, p. 11.

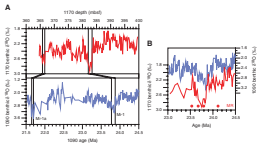

The Mi-1 event appears in benthic foraminiferal $\delta^{18}O$ records as a cold interval lasting from ~24.02 to 23.66 Ma, centering around a double peak of extremely heavy (cold) values from 23.89 to 23.79 Ma (cf. Billups et al., 2002). One important difference between this event at Site 1170 relative to Site 1090 (as well as 929) (Paul et al., 2000) is that the second peak appears to be as strong, if not even slightly stronger than the first peak. A second difference is that this double peak appears to begin and end later at Site 1170 (Fig. F2B). At Site 1170 timing of the Mi-1 event is constrained by four magnetostratigraphic datums across a depth of only 3.5 m, including one at 23.8 Ma, giving evidence for a strongly condensed section. It is this reversal at 23.8 Ma (onset of Subchron C6Cn.2n at 382.90 meters below seafloor [mbsf]), which is in conflict with an alignment of the Mi-1 double peak at both sites (23.88 Ma [383.36 mbsf] and 23.8 Ma [381.96 mbsf]). Matching the timing of the Mi-1a event at Site 1170 with Site 1090 provides two additional control points (Fig. F2A).

F3. Bio- and magnetostratigraphic data, p. 12.

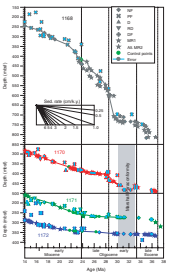

Additional information evident in the record of weight percent sand for Site 1170 indicates a change in the pattern of sedimentation (increase in the coarse fraction) between 406.69 and 405.34 mbsf (Fig. F4). This is consistent with the correlation indicated by the magnetostratigraphy (Fig. F3). The weight percent sand record further suggests placement of the Marshall Paraconformity (~32–29 Ma) (Fulthorpe et al.,

1996) somewhere between 476.66 and 463.61 mbsf (no samples) at a drop in average values (see also "Site 1171," p. 5, "Site 1172," p. 6, and "Site 1168," p. 6). This hiatus is common in sedimentary records from the southwest Pacific Ocean and is a logical explanation for an early Oligocene hiatus in the Leg 189 sites. At Site 1170 this hiatus is constrained by three biostratigraphic markers (33 Ma [478.5–460 mbsf] and 30.62/30.24 Ma [462.3–454.61 mbsf]) and one magnetic reversal (33.058 Ma [470 mbsf]) (Fig. F3). We use the center of the youngest datum (30.24 Ma; first occurrence [FO] of *Rocella vigilans*) for the purpose of interpolation downward from the last control point (Fig. F3).

These data raise an interesting conundrum in correlation, as one would not expect to find the isotope signature of a significant glacial event (Mi-1) with different ages at separated locations (i.e., they should occur at the same time worldwide), but the same is also true of magnetic reversal ages. Closer examination is required. See also more recent age model information in the papers by **Stickley et al.** (this volume) and Pfuhl et al. (in press).

Additional records of bulk $\delta^{13}C$ and benthic $\delta^{18}O$ and $\delta^{13}C$ presented in Figure F4 will be referred to in "Site 1171" below and "Site 1172," p. 6.

F4. Sand, carbonate, and benthic and bulk $\delta^{13}C$, Site 1170, p. 13.

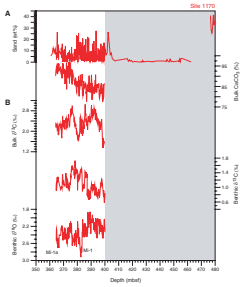

F5. Sand, carbonate, and benthic and bulk $\delta^{13}C$, Site 1171, p. 14.

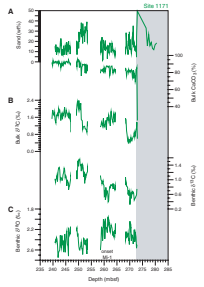

Site 1171

The biomagnetostratigraphy for Site 1171 suggests a transition from a heavily condensed Oligocene (sedimentation rates < 0.5 cm/k.y.) to slightly increased sedimentation rates in the Miocene (0.5–1 cm/k.y.) (Fig. F3). Unfortunately, magnetic reversals are less frequently observed than at Site 1170 and we fail to detect a complete Mi-1 event in the benthic $\delta^{18}O$ record (Fig. F5), but we do observe a number of characteristic markers in the records obtained.

Our oldest observation is a dramatic (~60%) and instantaneous (between 273 and 272.8 mbsf [279.68 and 279.48 meters composite depth (mcd)]) increase in $CaCO_3$ accompanied by a drop in weight percent sand similar to the one observed at Site 1170 (Fig. F4). We once again suggest that this transition marks the Marshall Paraconformity. This is in good accordance with six biostratigraphic datums (Fig. F3). We use the same diatom datum as at Site 1170 to mark the top of the hiatus at 30.24 Ma (FO of *R. vigilans*) and our suggested depth of 272.9 mbsf (error of datum = 274.32–272.74 mbsf). It is followed by a rapid transition to heavier values in both benthic and bulk $\delta^{13}C$ (269.36–269.16 and 269.16–268.56 mbsf) (Fig. F5). The lack of variability and the transition over 60 cm in the case of the bulk record suggests a strongly condensed section rather than a few hiatuses. We observe similar shifts in the $\delta^{13}C$ records at Site 1170 at ~401 mbsf (~26.9 Ma) and 398 mbsf (~26.34 Ma) followed by a strongly condensed interval ending at ~24.781 Ma (Fig. F4). Three biostratigraphic control points at Site 1171 suggest the same pattern for this site. Unfortunately, this interval is also marked by poor recovery. However, in order to relate these observations to the age model we decided to add control points centering on the two $\delta^{13}C$ increases and ignore the biostratigraphic datums.

The magnetic reversal at 268 mbsf, assigned an age of 24.118 Ma (onset of Subchron C6Cn.3n), implies a very strong increase in sedimentation rate, which appears most unlikely based on our present understanding of the sedimentary regime at all Leg 189 sites. Considering both poor recovery and low sedimentation rates before and after this datum, we suggest this datum also be ignored. A further control

point, which we place at 258.56 mbsf (23.88 Ma), is based on the increase in benthic $\delta^{18}O$, which we identify as the onset of the Mi-1 event (Fig. F5). The remainder of this event was not recovered during drilling of Hole 1171C (core gap at 258.80–253.84 mbsf). Connection of this and the previous control points are consistent with the biostratigraphy (Fig. F3).

Above this gap we observe a low in benthic $\delta^{13}C$ and matched increases in bulk $\delta^{13}C$ and $CaCO_3$ (251.90 and 251.06–250.86 mbsf) (Fig. F5). Based on similarities with Site 1170, we assign ages of 23.15 and 22.8 Ma (increase at Site 1170 between samples at 377.46 and 376.50 mbsf across a core gap) (Fig. F4). The ensuing low sedimentation rates lasting ~1 m.y. following the OMB at Site 1171 are consistent with biostratigraphic datums at this site and a similar trend at Site 1170. An additional control point is placed at 22.4 Ma (249.36 mbsf) based on correlation with the benthic $\delta^{18}O$ record at Site 1170. A last control point is placed at 21.7 Ma (240.23 mbsf) based on the benthic $\delta^{13}C$ record.

Two more gaps in recovery in Hole 1171C are evident at 268.10–264.88 and 248.90–247.38 mbsf.

Site 1172

Site 1172 has a greater number of magnetostratigraphic control points than Site 1171 across the interval studied (Fig. F3). However, the Oligocene interval is marked by very few additional biostratigraphic datums. We estimate that sedimentation resumes above the Marshall Paraconformity at 30.098 Ma (magnetic reversal onset of Subchron C11n.2n [358.6 mbsf]), but sedimentation rates remain very low, as suggested by three closely spaced magnetic reversals. As at Sites 1170 and 1171, we observe a sharp drop in weight percent sand at the Marshall Paraconformity (i.e., between 358.66 and 358.16 mbsf) (Fig. F6). This constrains placement of the hiatus to within 6 cm (358.66–358.60 mbsf). Our records suggest two additional control points based on correlation with Sites 1170 and 1171. At Site 1172 the bulk $\delta^{13}C$ record shows two strong increases (347.36–347.26 and 342.96–342.76 mbsf) (Fig. F6) that we match with the respective control points for the other two sites. Whereas these datum levels are close to the error given for two biostratigraphic datums, they are inconsistent with the magnetostratigraphy. However, in a strongly condensed section with potential hiatuses, identification of reversals is severely compromised.

We are confident in the placement of these two $\delta^{13}C$ datums and suggest two additional points based on similarities between the benthic $\delta^{18}O$ (onset of the Mi-1 event) and benthic $\delta^{13}C$ records from 344.47–344.27 and 342.56–342.46 mbsf, respectively (Fig. F6). The second control point is more difficult to define at Site 1170 where the decrease in benthic $\delta^{13}C$ occurs over a number of samples from 375.56 to 375.06 mbsf (Fig. F4). However, we place our control point based on the turning point in the $\delta^{13}C$ record. Two final control points are based on the benthic and bulk $\delta^{13}C$ records at 23.15 Ma (343.26 mbsf) and 21.79 Ma (339.86 mbsf).

Site 1168

Although the general trends observed in the records at Sites 1170–1172 reveal numerous similarities, we have difficulty in detecting

F6. Sand and bulk and benthic $\delta^{13}C$, Site 1172, p. 15.

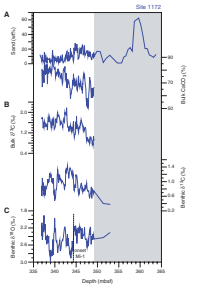

matching patterns at Site 1168 (Fig. F7). In this we are also constrained by lack of comparable data (i.e., the only stable isotopes available were measured on benthic foraminifers at very low resolution) (Dr. S. Schellenberg, pers. comm., 2002; but see also Pfuhl et al., in press). $CaCO_3$ was measured on the fine fraction only, but a comparison with bulk values at this site (Dr. C. Kelly, unpubl. data) and between bulk and fine values at Sites 1170–1172 suggest that the records can be overlaid (Fig. F7).

Our data reveal a strong transitional interval from ~765 to 735 mbsf marked by decreasing weight percent sand and organic carbon content, as well as increasing carbonate content (Fig. F8). We suggest that this interval marks the Eocene–Oligocene transition similar to Sites 1170–1172, possibly without the development of the Marshall Paraconformity at this rather protected site on the continental margin of Tasmania. Following this transition we note a number of changes in the biogenic and lithogenic composition of the coarse fraction (>63 µm) at this site (Fig. F9). The first two occur at ~699 and 538 mbsf. At ~429 mbsf we note the end of a strongly condensed interval (shipboard observation on benthic foraminifers). Between 405.22 and 404.98 mbsf the carbonate content increases (Fig. F8) followed by an increase in dissolution and weight percent sand at 386.23 mbsf (Fig. F9). All these datums are matched closely by changes in sedimentation suggested by the biomagnetostratigraphy based on magnetic reversal interpretation MR1 (Fig. F3).

If we assume the timing of the Mi-1 event recognized isotopically to be identical at all Leg 189 sites, we would have to tentatively place the peaks of this event at 23.9 Ma (420 mbsf) and 23.75 Ma (414 mbsf). This is consistent with the biomagnetostratigraphy (based on magnetic reversal interpretation MR1) within the error resulting from very low resolution (1.50 m) of measurements available at present. In comparison with the other three sites the changes in sedimentation rates across the Oligocene–Miocene transition are relatively strongest at this site. We suggest ignoring the planktonic foraminiferal datum at 22.8 Ma (379.60 mbsf; last occurrence [LO] of *Dentoglobigerina globularis*) because of its proximity to an event at 22.6 Ma (373.97 mbsf; FO of *Globoturborotalita woodi*) and place the FO of *Globoquadrina dehiscens* (planktonic foraminifers) at its upper limit of error (407.64 mbsf). The extreme increase in sedimentation rate at Site 1168 prior to the Oligocene–Miocene transition is fixed by two magnetic reversals and has to be accepted at this point.

All Sites

In Figure F10 we show the results of our measurements of lithologic and isotopic parameters at Sites 1170–1172 against their revised ages on the timescale of Cande and Kent (1992, 1995). Figure F11 shows a histogram of the sedimentation rates.

SUMMARY

The age models for the early Oligocene–early Miocene interval for ODP Sites 1168 and 1170–1172 were independently tested on the basis of a number of paleoceanographic data sets, including stable isotopes and carbonate content. With the exception of Site 1172, our integrated approach proves largely consistent with the magnetostratigraphic out-

F7. Overlap of bulk and fine-fraction carbonate, p. 16.

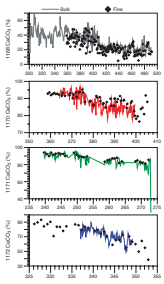

F8. Sand, carbonate, and TOC, Site 1168, p. 17.

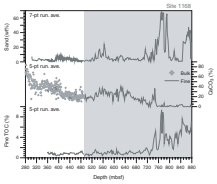

F9. Changes in sedimentation, Site 1168, p. 18.

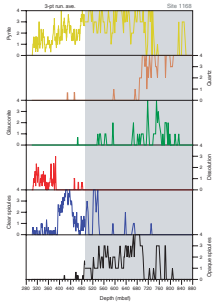

F10. Records used to define control points vs. revised ages, p. 19.

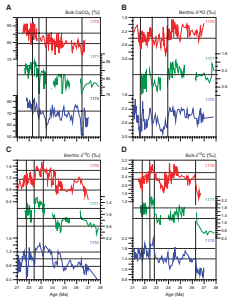

F11. Changes in sedimentation rates, p. 20.

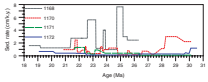

line (as of August 2002, we propose to follow magnetic reversal hypothesis 1 in the case of Site 1168). The development of these integrated age models forms the basis for a study of the hydrographic system around Tasmania. One of the questions addressed is the relationship between the sites and their respective location on the Pacific Ocean (Sites 1171–1172) or Indian Ocean (Sites 1168 and 1170) side of the South Tasman Rise.

Changes in sedimentation rates (Figs. **F3, F11**) suggest that Site 1168's location is rather different in character from Sites 1170–1172, due to its continental margin location. The Marshall Paraconformity in the early Oligocene is one of the most important hiatuses in the Southern Ocean region. The base of this hiatus is generally at ~33 Ma in deep-sea sections (Shipboard Scientific Party, 1999a, 1999b) and is at 32.4 Ma at the onland type location (Fulthorpe et al., 1996). Its duration at the type area is 3.4 m.y. (up to 29 Ma), but at Site 1122 it lasts until ~20 Ma (Shipboard Scientific Party, 1999a). Despite the significance of this hiatus for other sites, and here at Sites 1170–1172 from ~33 to 30 Ma, at Site 1168 it is apparently represented only by an interval of reduced sedimentation rate. Sedimentation rates return to high values throughout the Oligocene and Miocene.

Sites 1171 on the east South Tasman Rise and 1172 in the Tasman Sea are clearly most strongly affected by the Marshall Paraconformity. Even though the hiatus appears to end at ~30 Ma, sedimentation rates remain low for most of the Oligocene. At Site 1170 on the west South Tasman Rise, sedimentation in the early Oligocene is relatively high. However, this does change following the early/late Oligocene boundary, when we observe a decrease similar to but more pronounced than that at Site 1168. At Site 1168 we observe a change in the biogenic components of the sediment. The transition from opaque and sometimes branched spicules to clear, tiny, straight spicules with a canal might imply a change in water depth or ocean circulation. The Oligocene/Miocene boundary is marked by a strongly condensed section or small hiatus/core gap in Sites 1170–1172 from just before the boundary to ~22.8 Ma, but the overall decrease in sedimentation rate across this interval is greatest at Site 1168. The problem of the mismatch of the Mi-1 event (and/or the adjacent magnetic reversals) at Sites 1168 and 1170 requires closer investigation, as two key tenets of deep-sea stratigraphy appear to be in conflict.

ACKNOWLEDGMENTS

Special thanks go to Mike Hall, Patrizia Ferretti, James Rolfe, and Benoit Vautravers at Cambridge University for excellent sample preparation, and the Leg 189 time-team (the micropaleontologists and magnetic stratigraphers) for their efforts in providing the necessary age control. We would also like to thank Bob Carter and Ken Miller for their careful reviews and Clay Kelly for unpublished data.

This research used samples and/or data provided by the Ocean Drilling Program (ODP). The ODP is sponsored by the U.S. National Science Foundation (NSF) and participating countries under management of Joint Oceanographic Institutions (JOI), Inc. Research funding was provided through special ODP postcruise and small research grants by the UK Natural Environmental Research Council.

REFERENCES

Billups, K., Channell, J.E.T., and Zachos, J.C., 2002. Late Oligocene to early Miocene geochronology and paleoceanography from the subantarctic South Atlantic. *Paleoceanography,* 17:4–11.

Cande, S.C., and Kent, D.V., 1992. A new geomagnetic polarity time scale for the Late Cretaceous and Cenozoic. *J. Geophys. Res.,* 97:13917–13951.

————, 1995. Revised calibration of the geomagnetic polarity timescale for the Late Cretaceous and Cenozoic. *J. Geophys. Res.,* 100:6093–6095.

Exon, N.F., Kennett, J.P., Malone, M.J., et al., 2001. *Proc. ODP, Init. Repts.,* 189 [CD-ROM]. Available from: Ocean Drilling Program, Texas A&M University, College Station TX 77845-9547, USA.

Fulthorpe, C.S., Carter, R.M., Miller, K.G., and Wilson, J., 1996. The Marshall Paraconformity: a mid-Oligocene record of inception of the Antarctic circumpolar current and coeval glacio-eustatic lowstand. *Mar. Pet. Geol.,* 13:61–77.

Miller, K.G., Aubry, M.P., Khan, M.J., Melillo, A.J., Kent, D.V., and Berggren, W.A., 1985. Oligocene–Miocene biostratigraphy, magnetostratigraphy, and isotopic stratigraphy of the western North Atlantic. *Geology,* 13:257–261.

Paul, H.A., Zachos, J.C., Flower, B.P., and Tripati, A., 2000. Orbitally induced climate and geochemical variability across the Oligocene/Miocene boundary. *Paleoceanography,* 15:471–485.

Pfuhl, H.A., McCave, I.N., Schellenberg, S.A., and Ferretti, P., in press. Changes in Southern Ocean circulation in late Oligocene to early Miocene time. *In* Exon, N.F., Kennett, J.P., and Malone, M.J. (Eds.), *Cenozoic Paleoceanography and Tectonics in the Expanding Tasmanian Seaway.* Am. Geophys. Union, Geophys. Monogr.

Shackleton, N.J., and Hall, M.A., 1997. The late Miocene stable isotope record, Site 926. *In* Shackleton, N.J., Curry, W.B., Richter, C., and Bralower, T.J. (Eds.), *Proc. ODP, Sci. Results,* 154: College Station, TX (Ocean Drilling Program), 367–373.

Shackleton, N.J., Hall, M.A., Raffi, I., Tauxe, L., and Zachos, J., 2000. Astronomical calibration age for the Oligocene/Miocene boundary. *Geology,* 28:447–450.

Shipboard Scientific Party, 1999a. Site 1123: North Chatham Drift—a 20-Ma record of the Pacific Deep Western Boundary Current. *In* Carter, R.M., McCave, I.N., Richter, C., Carter, L., et al., *Proc. ODP, Init. Repts.,* 181, 1–184 [CD-ROM]. Available from: Ocean Drilling Program, Texas A&M University, College Station, TX 77845-9547, U.S.A.

————, 1999b. Site 1124: Rekohu Drift—from the K/T boundary to the Deep Western Boundary Current. *In* Carter, R.M., McCave, I.N., Richter, C., Carter, L., et al., *Proc. ODP, Init. Repts.,* 181, 1–137 [CD-ROM]. Available from: Ocean Drilling Program, Texas A&M University, College Station, TX 77845-9547, U.S.A.

Figure F1. Map of the South Tasman Rise and adjoining areas indicating the drill sites studied. Site 1169 was abandoned and is not discussed.

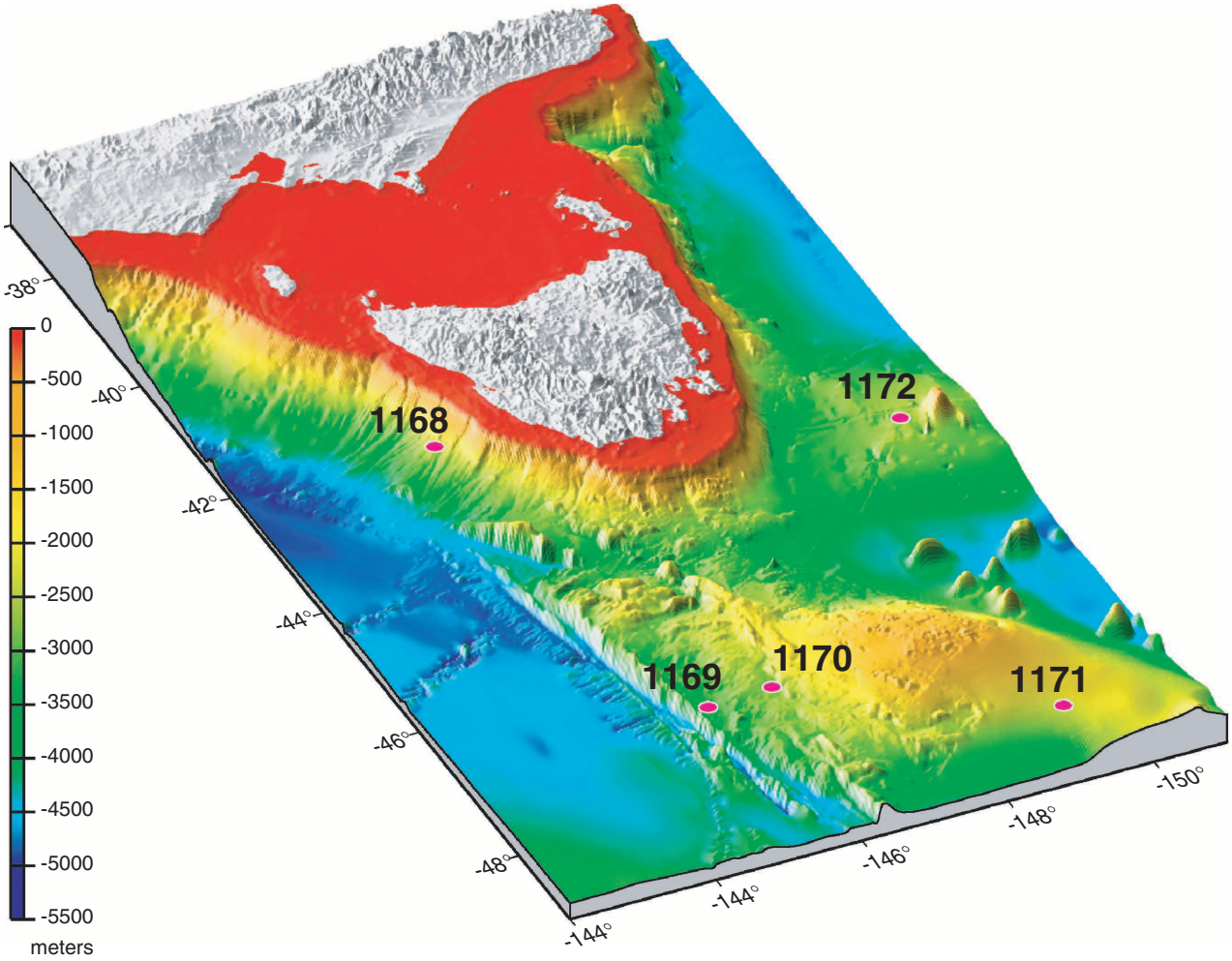

Figure F2. A. Comparison of the benthic stable isotope records for Sites 1170 and 1190 (Billups et al., 2002) across the late Oligocene–early Miocene providing the basis for matching up the Mi-1a and Mi-1 events. **B.** A detailed comparison of the Mi-1 events including the magnetic reversal points at Site 1170 show that the pattern of the characteristic double-peak of this event is different between sites. Ages are after Cande and Kent (1995). MR = magnetic reversal.

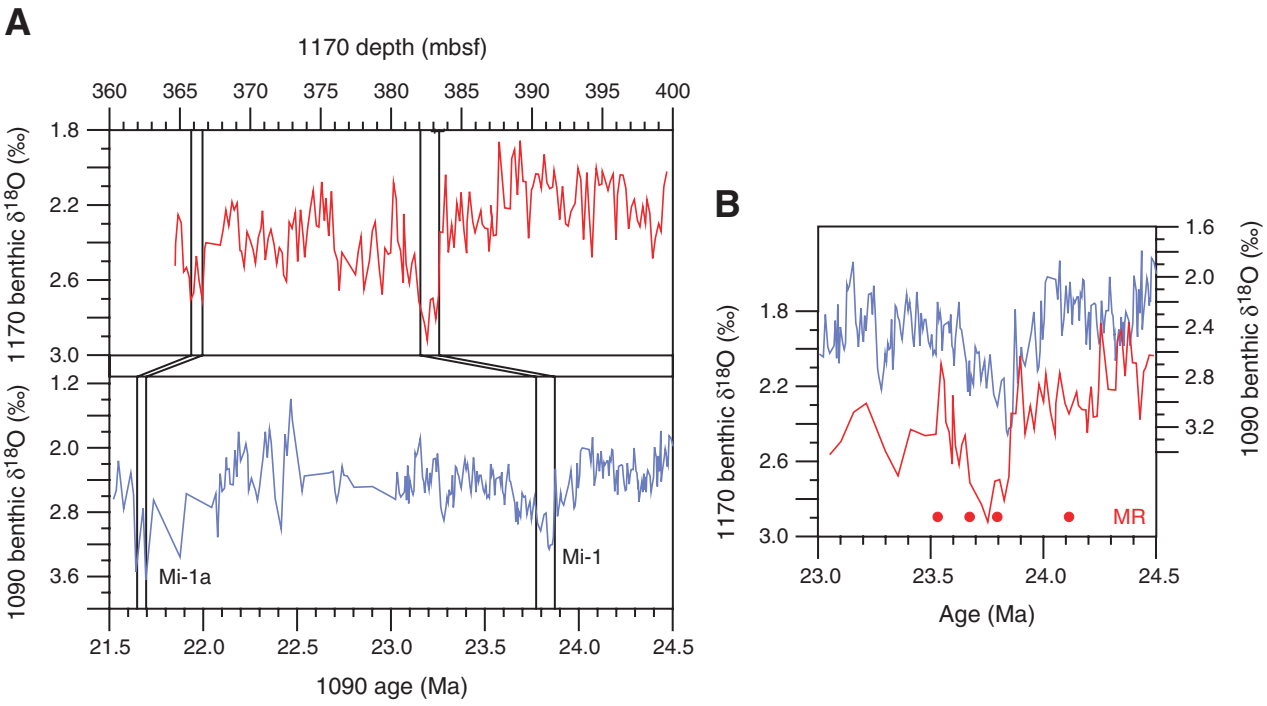

Figure F3. Bio- and magnetostratigraphic data for Sites 1168 and 1170–1172, as of August 2002 (errors given based on lower and upper samples confining biostratigraphic datums) (see also Pfuhl et al., in press; **Stickley et al.,** this volume), for the interval from 38 to 14 Ma including additional control points for the Oligocene and early Miocene interval based on similarities between the records (see Table **T1,** p. 21, and text for details). At all four sites we follow largely the sedimentation pattern suggested by the magnetostratigraphy (MR = magnetic reversals). Our control points are consistent within the magnetostratigraphic outline including a few biostratigraphic datums (NF = nannofossils, PF = planktonic foraminifers, D = diatoms, RD = radiolarians, and DF = dinoflagellates), with the exception of Site 1172. Here extremely low sedimentation rates suggest difficulties in identifying the magnetic reversals across the Oligocene/Miocene boundary. Our age models suggest there is no hiatus at the level of the Marshall Paraconformity at Site 1168, but a relatively strong reduction in sedimentation rate across the Oligocene/Miocene boundary (see text for discussion). Scales for all four sites are identical. Ages are after Cande and Kent (1995).

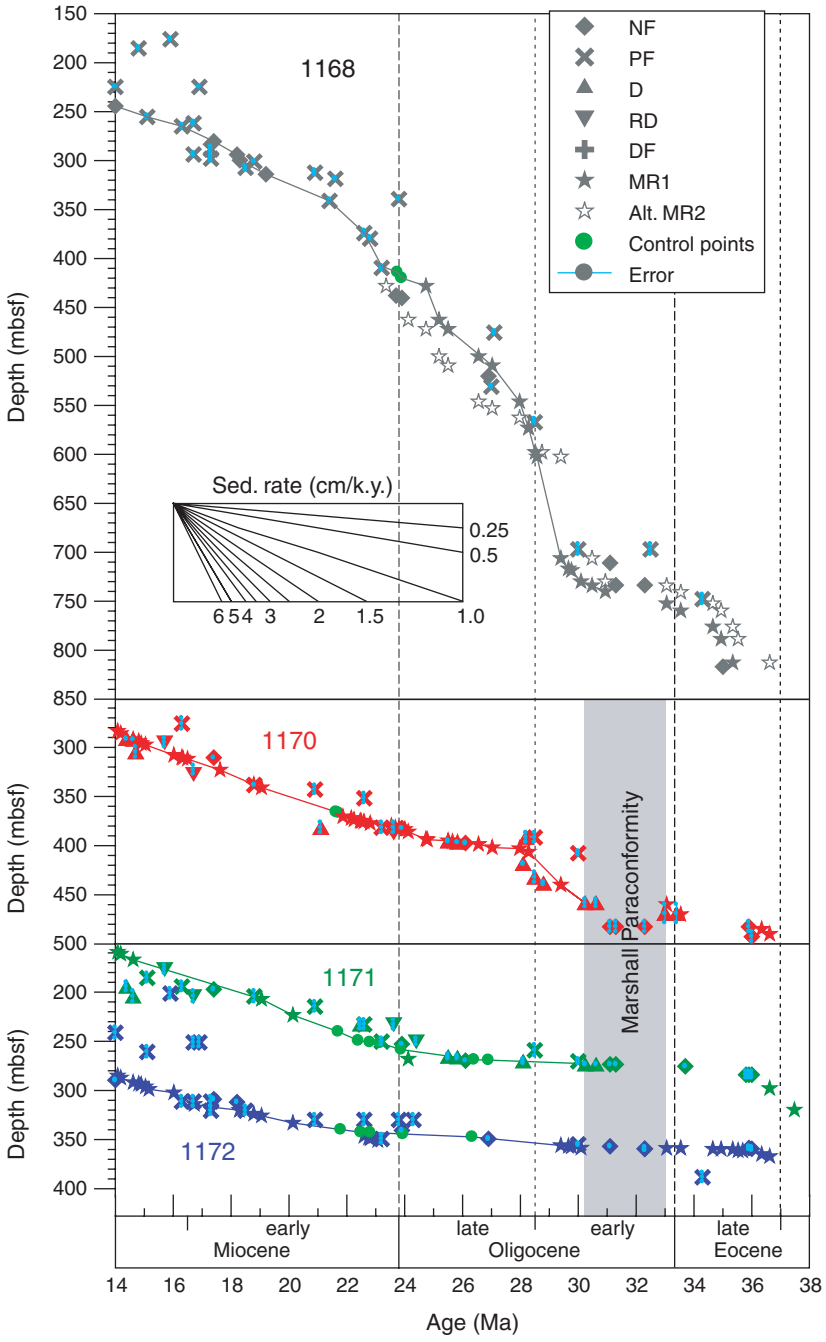

Figure F4. A. The record of weight percent sand (>63 µm) indicates two important changes between 476.66 and 473.61 mbsf (no samples) and 406.69 and 405.34 mbsf, while the carbonate content increases across the core gap from 377.46 to 376.50 mbsf. **B.** Increases in benthic and bulk $\delta^{13}C$ occur over a number of samples from ~401 to 398 mbsf, while a decrease in benthic $\delta^{13}C$ from 375.56 to 375.06 mbsf appears more gradual.

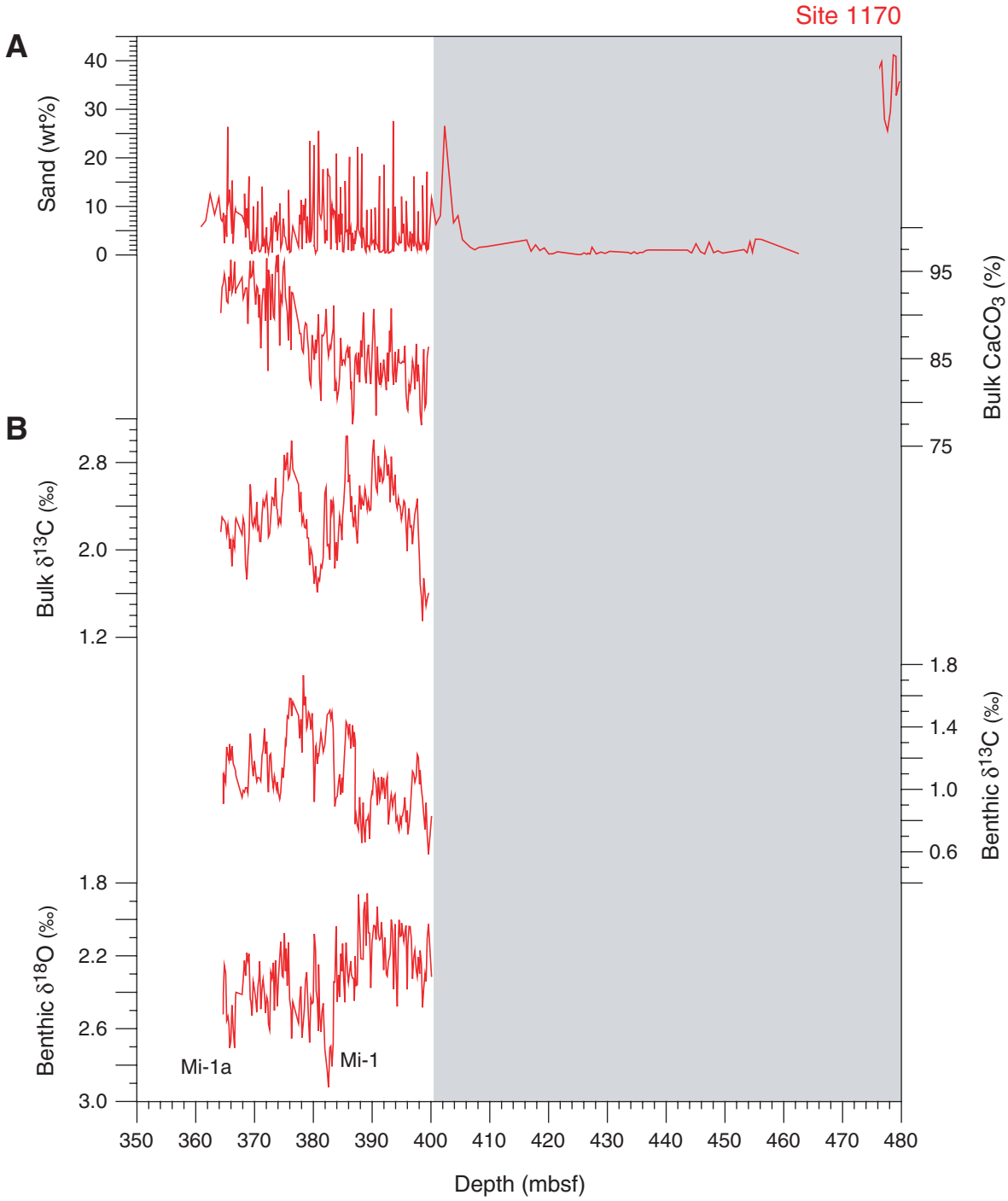

Figure F5. A. The record of weight percent sand experiences a strong decrease matching the increase in carbonate content from 273 to 272.8 mbsf (279.68–279.48 mcd). A second increase in carbonate content occurs at 252.06–250.86 mbsf. **B.** Increases in benthic and bulk $\delta^{13}C$ occur over a number of samples from 269.36 to 269.16 and 269.16 to 268.56 mbsf. **C.** The strong increase in benthic $\delta^{18}O$ at 258.65 mbsf is identified as the onset of the Mi-1 event.

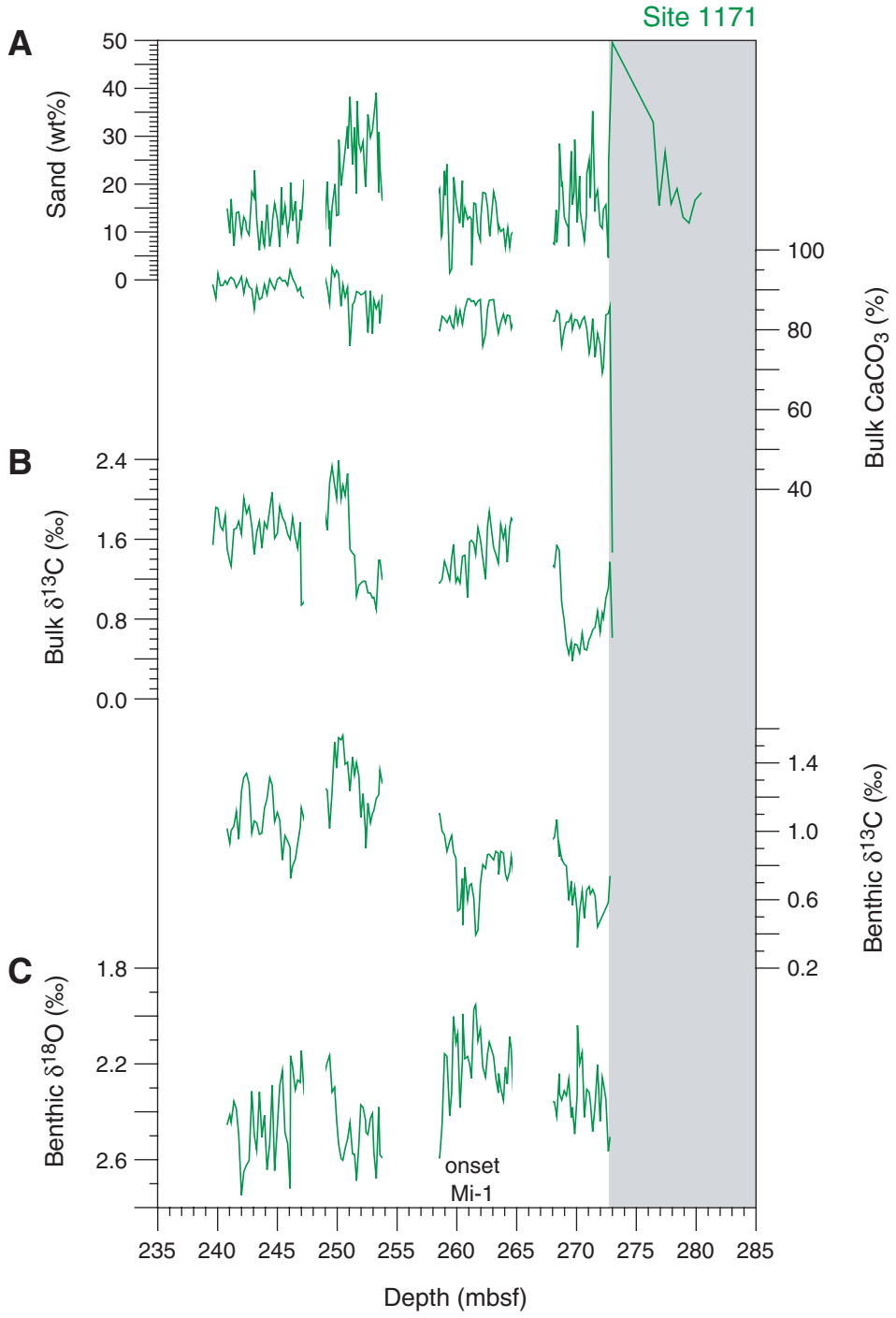

Figure F6. A. The record of weight percent sand experiences a sharp drop at ~358.60 mbsf. **B.** The bulk $\delta^{13}C$ record shows two strong increases at 347.36–347.26 and 342.96–342.76 mbsf, while the benthic $\delta^{13}C$ record experiences a strong decrease at 342.56–342.46 mbsf. **C.** A strong increase in the benthic $\delta^{18}O$ record at 344.37–344.27 mbsf resembles the onset of the Mi-1 event at the other sites.

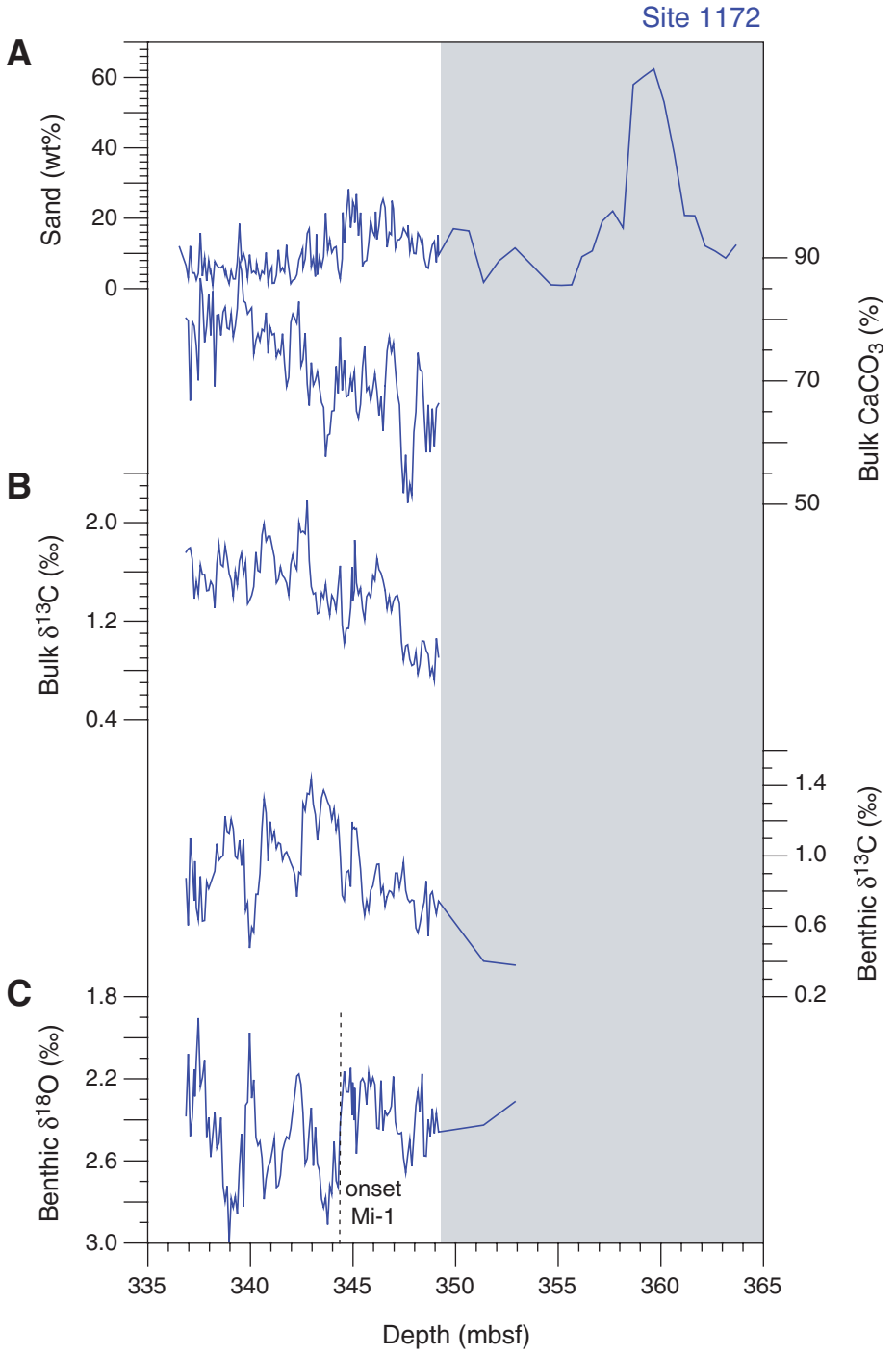

Figure F7. Comparison of records of carbonate content obtained on the bulk and fine fraction of the sediment showing strong overlap.

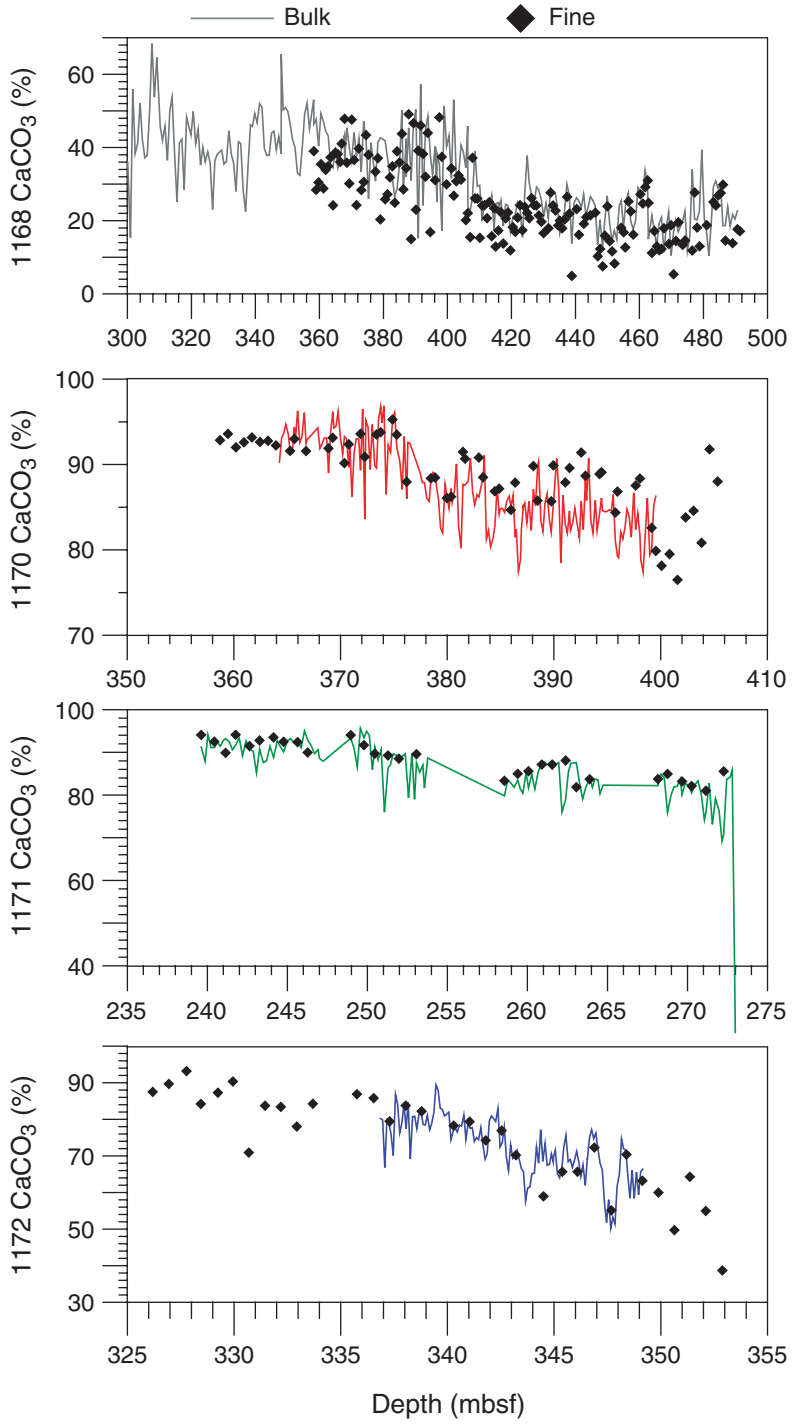

Figure F8. Sand, carbonate content, and organic carbon content (TOC) indicate a strong transitional interval from ~765 to 735 mbsf. An increase in carbonate content at 405.33–404.98 mbsf is closely followed by a decrease in sand at 386.23 mbsf.

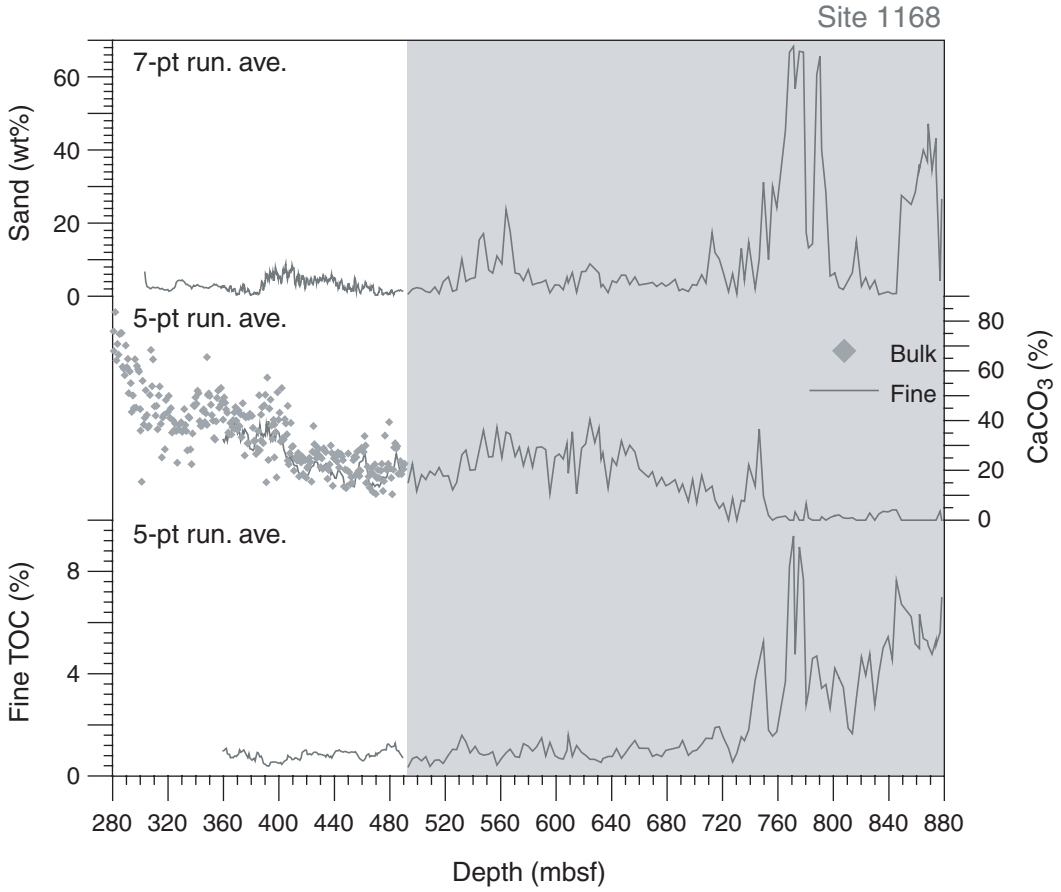

Figure F9. Biogenic and lithogenic composition of the coarse fraction (>63 µm) of the sediment suggests two changes in sedimentation at ~699 and 538 mbsf. An increase in dissolution occurs at 386.23 mbsf.

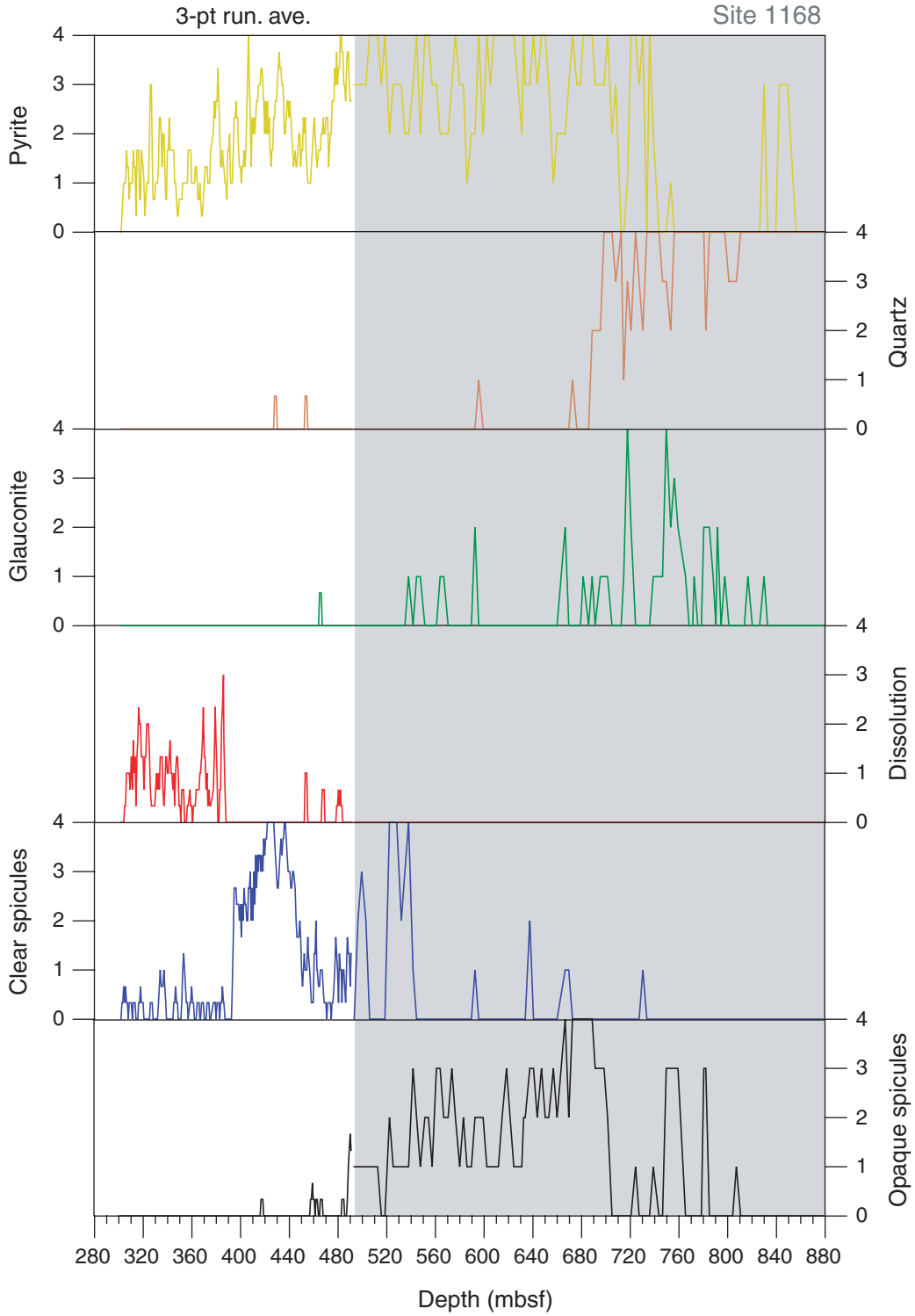

Figure F10. A–D. Comparison of the different records used in defining additional control points between Sites 1170–1172 against their revised ages. The records reveal good matches at different times depending on the parameter. Ages from Cande and Kent (1995).

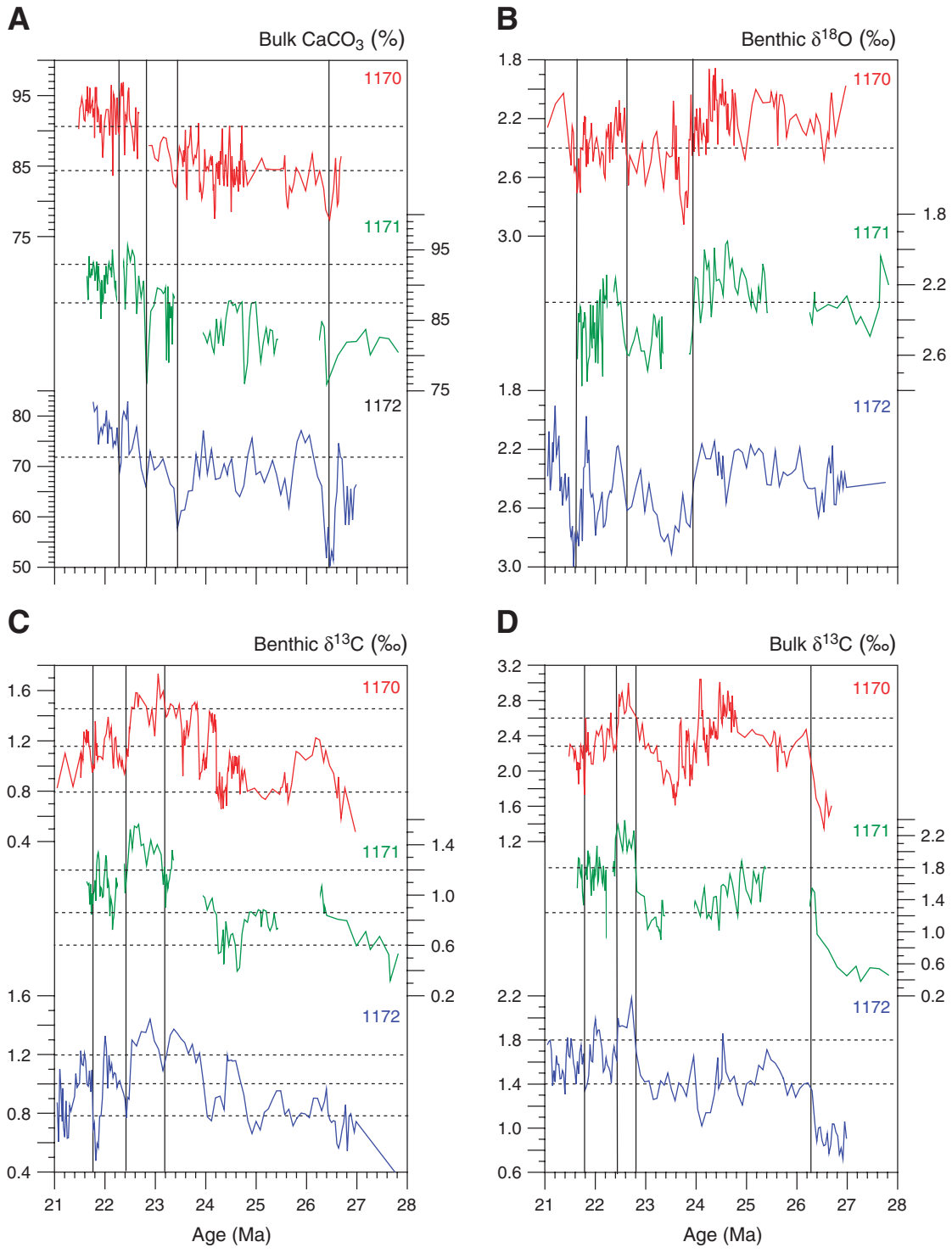

Figure F11. Histogram depicting changes in sedimentation rates based on interpolation between datums listed in Table T1, p. 21. Ages from Cande and Kent (1995).

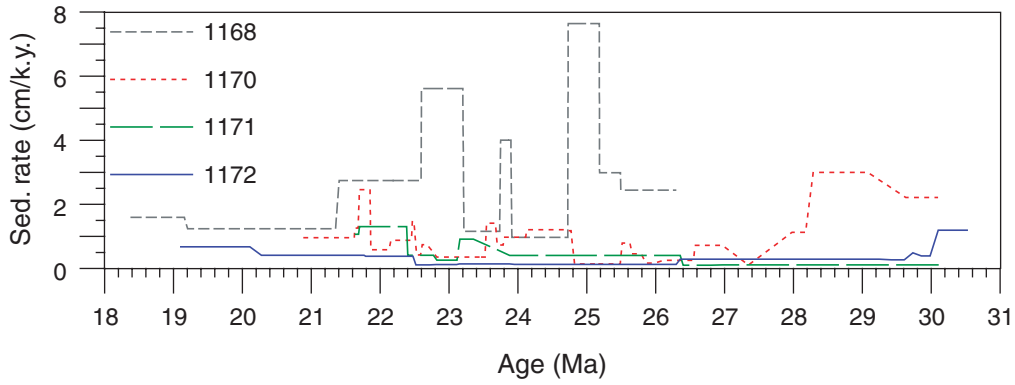

Table T1. Overview of the fossil, magnetic reversal and additional datums used in developing the age models for the Leg 189 sites.

Age (Ma)	Event	1170 (mbsf)	Age (Ma)	Event	1171 (mbsf)	Age (Ma)	Event	1172 (mbsf)	Age (Ma)	Event	1168 (mbsf)
14.076	MR-Onset C5ACn	283.50	14.076	MR-Onset C5ACn	159.35	14.076	MR-Onset C5ACn	285.20	14.000	NF-FO *Triquetrorhabdulus rugosus*	244.30
14.178	MR-Termination C5ADn	286.00	14.178	MR-Termination C5ADn	161.30	14.178	MR-Termination C5ADn	287.30	15.100	PF-FO *Orbulina suturalis*	255.26
14.380	D-FO *Actinocyclus ingens* var. *nodus*	291.42	14.612	MR-Onset C5ADn	167.20	14.612	MR-Onset C5ADn	291.90	16.300	PF- FO *Praeorbulina curva*	264.90
14.612	MR-Onset C5ADn	292.00	19.048	MR-Termination C6n	207.20	14.800	MR-Termination C5Bn.1n	293.30	17.400	NF-FO *Calcidiscus premacintyrei*	280.35
14.800	MR-Termination C5Bn.1n	294.00	20.131	MR-Onset C6n	223.50	14.888	MR-Onset C5Bn.1n	293.90	18.200	NF-FO *Sphenolithus heteromorphus*	293.80
14.888	MR-Onset C5Bn.1n	296.00	21.700	1170-benthic $\delta^{13}C$	240.23	15.034	MR-Termination C5Bn.2n	296.30	18.300	NF-LO *Sphenolithus belemnos*	299.55
15.034	MR-Termination C5Bn.2n	297.50		Top of gap	247.38	15.155	MR-Onset C5Bn.2n	298.80	19.200	NF-FO *Sphenolithus belemnos*	313.90
16.014	MR-Termination C5Cn.1n	308.00		Bottom of gap	248.90	16.014	MR-Termination C5Cn.1n	302.30	21.400	PF-LO *Tenuitella munda*	341.10
16.293	MR-Onset C5Cn.1n	310.50	22.400	1170-benthic $\delta^{18}O$	249.36	16.726	MR-Onset C5Cn.3n	314.10	22.600	PF-FO *Globoturborotalita woodi*	373.97
16.327	MR-Termination C5Cn.2n	311.00	22.800	1170-bulk $\delta^{13}C$	251.00	17.277	MR-Termination C5Dn	316.90	23.200	PF-FO *Globoquadrina dehiscens*	407.64
16.488	MR-Onset C5Cn.2n	312.00	23.150	1170-benthic $\delta^{13}C$	251.90	18.281	MR-Termination C5En	320.20	23.750	1170-Mi1 peaks	414.00
17.615	MR-Onset C5Dn	323.00		Top of gap	253.84	18.781	MR-Onset C5En	324.00	23.900	1170-Mi1 peaks	420.00
18.781	MR-Onset C5En	338.00		Bottom of gap	258.50	19.048	MR-Termination C6n	325.80	24.730	MR-1-Termination C7n.1n	428.05
19.048	MR-Termination C6n	341.00	23.880	1170-benthic $\delta^{18}O$	258.56	20.131	MR-Onset C6n	333.10	25.183	MR-1-Onset C7n.2n	462.65
21.634	1090 Mi-1a	365.76		Top of gap	264.88	21.790	1170-bulk $\delta^{13}C$	339.86	25.496	MR-1-Termination C7An	472.00
21.700	1090 Mi-1a	366.59		Bottom of gap	268.10	22.490	1170-benthic $\delta^{13}C$	342.51	27.027	MR-1-Termination C9n	509.35
21.859	MR-Onset C6AAn	370.50	26.400	1170-bulk $\delta^{13}C$	268.76	22.810	1170-bulk $\delta^{13}C$	342.86	27.972	MR-1-Onset C9n	546.20
22.151	MR-Termination C6AAr.1n	372.20	26.900	1170-benthic $\delta^{13}C$	269.26	23.150	1170-benthic $\delta^{13}C$	343.26	28.283	MR-1-Termination C10n.1n	572.90
22.459	MR-Termination C6AAr.2n	374.90	30.240	D-FO *Rocella vigilans*-~top MPC	272.90	23.950	1170-benthic $\delta^{18}O$	344.37	28.512	MR-1-Onset C10n.1n	597.80
22.493	MR-Onset C6AAr.2n	375.40				26.340	1170-bulk $\delta^{13}C$	347.31	28.578	MR-1-Termination C10n.2n	602.45
22.588	MR-Termination C6Bn.1n	375.80				29.401	MR-Termination C11n.1n	356.10	29.401	MR-1-Termination C11n.1n	706.10
	Top of gap	376.58				29.662	MR-Onset C11n.1n	356.80	29.662	MR-1-Onset C11n.1n	716.70
22.804	MR-Termination C6Bn.2n-bottom of gap	377.40				29.765	MR-Termination C11n.2n	357.30	29.765	MR-1-Termination C11n.2n	718.48
23.535	MR-Onset C6Cn.1n	380.00				30.098	MR-Onset C11n.2n-~top MPC	358.60	30.098	MR-1-Onset C11n.2n	729.90
23.677	MR-Termination C6Cn.2n	382.00							30.479	MR-1-Termination C12n	733.95
23.800	MR-Onset C6Cn.2n	382.90							30.939	MR-1-Onset C12n	740.00
24.118	MR-Onset C6Cn.3n	386.00									
24.730	MR-Termination C7n.1n	393.40									
24.781	MR-Onset C7n.1n	394.00									
25.496	MR-Termination C7An	395.00									
25.648	MR-Onset C7An	396.20									
25.823	MR-Termination C8n.1n	397.00									
26.100	NF-LO *Chiasmolithus altus*	397.46									
26.554	MR-Onset C8n.2n	398.60									
27.027	MR-Termination C9n	402.00									
27.972	MR-Onset C9n	403.00									
28.283	MR-Termination C10n.1n	406.50									
29.401	MR-Termination C11n.1n	440.00									
30.240	D-FO *Rocella vigilans* - ~top MPC	458.55									

Notes: FO = first occurrence, LO = last occurrence. D = diatom, DF = dinocyst, NF = nannofossil, PF = planktonic foraminifer, RD = radiolarian. MR = magnetic reversal. MPC = Marshall Paraconformity. Gap = recovery gap.